

# Real-Time Digital Processing of GPS Measurements for Transmission Engineering

Chris Mensah-Bonsu, *Member, IEEE*, and Gerald Thomas Heydt, *Fellow, IEEE*

**Abstract**—The global positioning system (GPS) is a state-of-the-art timing and positioning system based on 24 or more satellites launched and maintained by the US government. Power engineering applications based on GPS include phasor measurement, positioning applications, such as surveying and mapping, and potentially in deriving real-time data on transmission lines that will allow them to be loaded to a dynamic (thermal or security) limit. Inherent errors in GPS technologies are discussed, and the differential GPS method is described for accuracy enhancement. Further digital-processing needs are necessary for meeting the accuracy requirements of certain specific applications. The focus of this paper is on the digital signal processing (DSP) of differential-GPS (DGPS) measurements. The paper describes a methodology for further improving DGPS altitude measurements for the purpose of accurate determination of high-voltage overhead conductor sag. The Haar wavelet transforms (HWT) and least-squares parameter estimation (LSPE) techniques are considered.

**Index Terms**—Dynamic thermal-line rating, GPS, least-squares parameter estimation, overhead conductor sag, transmission engineering, wavelet analysis.

## I. INTRODUCTION

THE global positioning system (GPS) is a positioning and timing system based on 24 satellites in operation, launched and maintained by the U.S. government. Each satellite orbits the Earth in approximately 12 h. Implemented initially with military applications in mind, the GPS/DGPS technology is highly reliable. Various engineering and military applications of the GPS and its basic technological concepts are described in [3], [4], [6], [18]. The essence of the GPS technology is a receiver clock offset and three-dimensional (3-D) position of GPS receivers, which are determined from measured satellite-to-receiver ranges called *pseudorange*. The pseudorange is based on four or more GPS satellite signal reception. For certain national security considerations, the GPS technology had original intentional inserted error known as selective availability (SA). In 2000, an SA error of approximately  $0.2 \mu\text{s}$  (60 m) was removed [21]. Errors due to the propagation of the signals from GPS satellites, errors in solving the system of pseudorange equations, and other errors occur. The presence of bad GPS measurement data could be attributed to a variety of sources, some of which are not fully understood. The momentary loss of some GPS satellites from view will negatively impact the measurement accuracy. Also, interference and signal reflections degrade

accuracy. In addition, the ambient noise impacts solution accuracy. Other error mechanisms may also create single datum values that are erroneous. One way to reduce these errors involves the comparison of a GPS position calculation with that at a known surveyed position. In this way, an error or a difference is generated which is then used as a correction. The concept is called differential GPS [3] and the technology is further denominated depending on the collection of the final position result at the surveyed base station (*direct DGPS*) or the “rover” remote station (*inverse DGPS*). More recently, there has been recommendations to add an additional frequency to the system. This is intended to improve the accuracy of civilian GPS applications. The DGPS operation offers significant position accuracy improvement over standard GPS. DGPS compensation greatly attenuates errors common to all local receivers in use. However, spatial correlation of atmospheric delays could cause the DGPS position accuracy to deteriorate with increasing distance between the reference and rover receivers. Equation (1) describes the autocorrelation function,  $R(d)$  between two DGPS receiver points separated by a distance  $d$  of correlation distance  $D$  and variance  $\sigma^2$  as [7],

$$R(d) = E(x_1, x_2) = \sigma^2 e^{(-d/D)} \quad (1)$$

where,  $x_1$  and  $x_2$  are the respective pseudorange errors at receiver positions one and two.

The following accounts for the increase use of DGPS: nanosecond-order precise time tagging capability (accuracy), compactness, portability, low cost, and around-the-clock operation in all weather conditions anywhere on Earth. DGPS has been used for different applications including dispatching/fleet management, emergency tracking, offshore exploration, and agriculture [3].

The main applications of GPS technology in power engineering have been in

- surveying;
- mapping;
- system protection;
- phasor measurement in real time.

In addition, recently, DGPS has been proposed for the measurement of overhead conductor sag in transmission circuits [1]. In that application, the main concept was the use of a DGPS-based instrument to accurately estimate the position of a point on the overhead conductor in a critical transmission-line span. The goal was to convert this conductor sag data to a dynamic (real-time) thermal rating of the line [1], [2], [8], [10], [11], [18]. The main results reported in this paper were obtained in prototyping the overhead conductor sag instrument. The use of GPS

Manuscript received September 29, 2000; revised July 17, 2002. This work was supported by the Arizona Public Service, AZ, Entergy in New Orleans, and the National Science Foundation Power Systems Engineering Research Center (PSERC).

The authors are with Arizona State University, Tempe, AZ 85287-5706 USA. Digital Object Identifier 10.1109/TPWRD.2002.803803

technology for phasor measurements and surveying in power engineering is well known: and these technologies do not have problems in accurate measurements of time and horizontal (i.e.,  $x - y$ ) position. The measurement of vertical position (i.e.,  $z$ ), however, is more problematic because some compromises were made in the GPS design to attain accuracy in  $x - y$  measurements. For this reason, the remaining focus of this paper relates to the DSP of vertical DGPS measurements for transmission engineering applications.

## II. DIGITAL PROCESSING OF GPS DATA

The GPS technology is heavily based on DSP. The pseudorandom signals from the GPS system are decoded, converted to pseudorange data, and solved for position and time at the receiver—all digitally. Evidence about the error in raw GPS measurement data has been reported since the inception of the technology more than two decades ago. The measurement errors can be traced to various sources including multipath, ionospheric, tropospheric effects, and clock offset [3], [4]. A distribution of errors that affect the  $x$ ,  $y$  and  $z$  positioning accuracy due to specifically selected factors are provided in Table I.

DGPS measurement errors ( $x$ ,  $y$ ,  $z$ ) in the order of 15 m and beyond are not unusual in some applications. In order to improve the measurement accuracy, postprocessing of the raw measurement data using appropriate engineering and DSP tools are therefore often inevitable. The accuracy requirement of DGPS data is application, device, and base-rover receiver separation distance dependent. Table II shows comparison of typical GPS and DGPS measurements above *ellipsoid* (vertical position, similar to mean sea level, a grade benchmark) for selected conditions based on field trials of more than 3500 s of measurements using a ten-channel GPS instrument. Various DGPS measurements were obtained experimentally using 12- and ten-channel DGPS receivers at a presurveyed position in Tempe, AZ, at an altitude of approximately 359 m above mean sea level. The readings were taken at the rate of one reading per second. These measurements were taken to illustrate the accuracy improvement using DGPS.

Differentially corrected GPS data can be appropriately transmitted at a desired set time interval to reduce processing burden. DGPS readings for ten distinct elevations (stations), collocated in longitude and latitude, were taken to validate known altitudes. The altitude difference between the stations was varied from 0.10 m to 1.0 m for the test site illustrated in Table III. An average of 1600 (26 min) readings per station were taken. Table III shows the statistical data analysis based on raw DGPS measurements and the respective filtered data using 12-channel DGPS receivers. In these tests, the effect of electric fields near 230-kV overhead lines is tested.

In Table III, the confidence interval, ( $CI$ ) is defined as

$$CI = \bar{z} \pm \beta (\sigma_z / \sqrt{n}) \quad (2)$$

where,  $\bar{z}$  is the mean of  $n$  number of samples of raw or filtered data and  $\sigma_z$  is the respective standard deviation. The constant coefficient  $\beta$  is dependent on the probability for which the sample mean lies within the confidence interval (e.g.,  $\beta =$

TABLE I  
ERROR DISTRIBUTION IN METERS [3], [4]

Error source	GPS	DGPS
Multipath	0.6	0.6
Ephemeris	2.5	0
Troposphere	0.5	0.2
Ionosphere	5.0	0.4

TABLE II  
STATISTICAL ANALYSIS OF GPS/DGPS MEASUREMENT OF ALTITUDE UNDER CONTROLLED CONDITIONS (TEMPE, AZ, TEN-CHANNEL RECEIVER)

Parameter	GPS	DGPS
$\sigma$	34.55 m	3.14 m
$\mu$	371.32	371.32
Median	372.53	372.11
Mode	386.00	372.11

TABLE III  
EFFECT OF BAD DATA MODIFICATION, DATA TAKEN 14-ft. DIRECTLY UNDER 230-kV LINES (TEMPE, AZ, APPROXIMATE ELECTRIC FIELD STRENGTH 0.3112-kV/cm, 12-CHANNEL RECEIVER)

DGPS sample parameters				Statistical parameter for DGPS measurements		
Data type	Station	Size $n$	$z$ (m)	$\bar{z}$ (m)	$\sigma_z$ (m)	90 % CI (m)
Filtered	3	1696	359.7	359.4	0.3	359.46-359.48
	4	1654	359.7	359.43	0.3	359.42-359.45
	6	997	360.5	360.39	0.3	360.38-360.41
	9	1780	359.7	359.93	0.2	359.92-359.94
	10	1310	359.5	359.80	0.3	359.79-359.82
Raw measurements	3	1696	359.7	359.30	1.8	359.40-359.54
	4	1654	359.7	359.47	1.8	359.36-359.51
	6	997	360.5	360.77	1.3	360.33-360.46
	9	1780	359.7	359.83	1.2	359.88-359.98
	10	1310	359.5	359.85	1.5	359.74-359.87

1.9600 for  $CI = 95\%$ ). Note that  $\sigma_z$  in Table III is improved (reduced) in the case of statistical analysis using the filtered (DSP) data compared to that of the measured raw data. Consequently, the  $CI$  is narrowed, respectively, as shown in Table III.

The main DSP techniques considered are shown in Fig. 1. Also illustrated are bad data identification and rejection (based on a  $\mu$ -calculation and  $\pm 1\sigma$  rejection), and three other estimating procedures: moving window time averaging, least-squares state estimation, and wavelet spectrum calculation and analysis. Various combinations of these methods are illustrated in Fig. 1. Even though options one and three in Fig. 1 yield better results compared with that of the raw DGPS data, their performance was not closer to that of options two and four. The results of LSPE and HWT analysis (i.e., options two and four) are presented in this paper. These are found to be

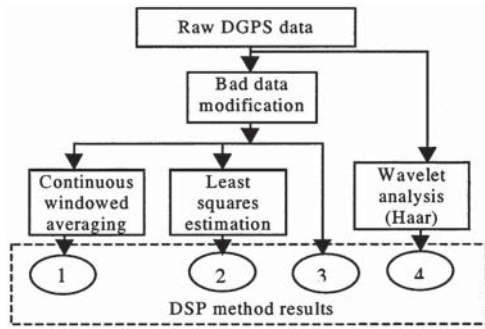


Fig. 1. Selected DSP methods.

most applicable for the DSP of DGPS vertical positioning data in a 60-Hz electric field.

### III. LEAST-SQUARES PARAMETER ESTIMATION

The concept of weighted LSPE is an old one. The method applied here is based on the usage of measurements,  $z$  of the vertical position taken from the physical process to obtain parameter vector  $x$ . Denoting the estimate of  $x$  as  $\hat{x}$ , the weighted LSPE algorithm is

$$z = Hx \quad (3)$$

$$\hat{x} = (\sqrt{W}H)^+ \sqrt{W}z \quad (4)$$

where  $(\bullet)^+$  denotes the Moore–Penrose pseudoinverse of a matrix [5], [20]. The matrix  $W$  is a weighting factor selected to maximize the usage of the most accurate measurement data. The measurement residual  $J(x)$  is described by

$$\min_x J(x) = \sum_{i=1}^{N_m} \frac{[z_i - (x)]^2}{\sigma_i^2} \quad (5)$$

where  $z_i$  is the  $i$ th measured quantity,  $x$  is the true value being measured by the  $i$ th measurement,  $\sigma_i^2$  is the variance for the  $i$ th measurement, with  $N_m$  being the number of sample measurements.

In this application, vector  $z$  is the measured altitudes using DGPS and  $x$  are the true altitude positions of the remote DGPS receiver. In trying to capture the nonlinear behavior of the error, the LSPE method adopted is formulated as

$$\hat{z}(n) = Ax(n) + By(n) + Cz(n) + Dx^2(n) + Ey^2(n) + Fz^2(n) \quad (6)$$

where  $x(n)$ ,  $y(n)$ ,  $z(n)$  are the sampled readings at certain times that produce the corresponding vertical measurement estimation  $\hat{z}(n)$ . Using the set of measurements  $x(n)$ ,  $y(n)$ ,  $z(n)$  taken for a set of known (i.e., controlled) altitude  $z_o$  and replacing  $\hat{z}(n)$  with  $z_o$ , (6) can be expressed in matrix form as follows:

$$Z_{\text{known}} = X\Theta \quad (7)$$

where  $\Theta = [A \ B \ C \ D \ E \ F]^T$  are determined using measurements corresponding to a known set of  $z_o$ . Thus, the parameters  $[A, B, C, D, E, F]$  are computed using simple-state estimation concept. One formulation involves the Moore–Penrose pseudoinverse of the matrix  $X$ .

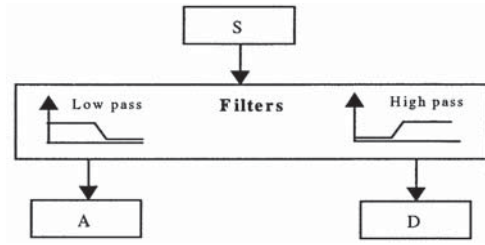


Fig. 2. Basic level of wavelet transform filtering process.

### IV. WAVELET ANALYSIS OF DGPS DATA

A wavelet may be described as a waveform of effectively limited duration that has an average value of zero but nonzero integral of the square. Unlike Fourier analysis, which consists of breaking up a signal into sine waves of various frequency components, the wavelet analysis decomposes a signal into shifted and scaled versions of the mother wavelet. This produces a time-scaled view of a signal. Wavelet analysis provides an alternative method for reconstructing and decomposing a given signal  $f(t)$ , into its constituent parts. Hence, it can provide information about signal patterns and behavior, or capture the location of local oscillations that represent a particular feature at a specific frequency level. Thus, the technique is capable of revealing data trends and discontinuities.

There is a volume of literature on the subject of wavelet transforms and their applications. Some selected few are given in [12]–[17]. The dilation and translation features of a wavelet transform can be described by a set of functions of the form

$$\psi_{ab}(x) = |a|^{-1/2} \psi\left(\frac{x-b}{a}\right) \quad (8)$$

representing a set of functions formed by dilations, that are controlled by a positive real number  $a \in R^+$  and translations that are controlled by the real number  $b \in R$ , of a single function  $\psi(x)$ , which is also known as the mother wavelet. The mother wavelet appears as a local oscillation. In (8), the dilation parameter  $a$  controls the width and rate of the local oscillation and, hence, can be thought of intuitively as controlling the frequency of  $\psi_{ab}(x)$ . The translation parameter,  $b$  moves the wavelets throughout the domain. The continuous wavelet transform (CWT) of a signal  $f(t)$  is also described in (9) as the integral of the signal multiplied by a scaled, shifted version of the wavelet function  $\psi$ ,

$$C_w(\text{scale}, \text{position}) = \int_{-\infty}^{\infty} f(t) \psi(\text{scale}, \text{position}, t) dt. \quad (9)$$

The results of the CWT are many wavelet coefficients  $C_w$ . These coefficients are functions of scale and position. The constituent wavelets of the original signal can be regenerated by summing the product of each coefficient and the appropriate scaled and shifted wavelet. The identity of most signals, can be traced to a low-frequency content (“approximation”) of the measurement. The high-frequency content (“detail”), on the other hand, imparts flavor [14]. In wavelet transform analysis, the approximation  $A$  as shown in the basic filtering process illustrated in Fig. 2 is the high-scale, low-frequency (i.e., identity) components of the given signal. The details  $D$  are the low-scale, high-frequency (flavor or nuance) components.

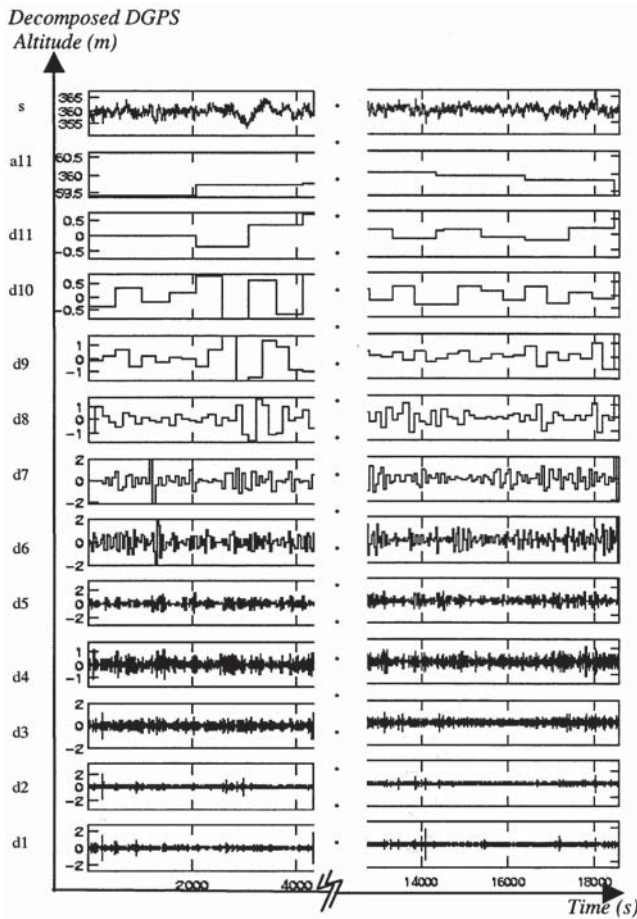


Fig. 3. Decomposed DGPS vertical position signal using HWT.

In Fig. 2, the original signal passes through two complementary filters and emerges as two signals. The scaling function is similar to the wavelet function and, can be determined by the lowpass filters. Therefore, it is associated with the approximation “ $A$ ” of the wavelet decomposition. In this paper, the approximation component of the DGPS signal is extracted and used for data analysis.

Wavelets have been applied in a variety of engineering and science applications where measurement accuracy is to be improved. In this paper, the application area is DGPS technology for overhead conductor sag measurement. The distinctive nature of the data under analysis requires the use of the Haar wavelet transform as a postprocessing technique to enhance the accuracy of the raw DGPS measurement data. Wavelet transforms can be used to compress or denoise a signal without appreciable degradation hence, unlike the LSPE method, the use of the HWT for data analysis does not require preidentification and modification of bad data from the raw (original) DGPS signal.

Fig. 3 shows the decomposition of the raw DGPS measurement data,  $s$ , using the HWT. The signal represents wavelet components of 12 subsignal levels for the ten different measured stations. In this case, a level 11 ( $n = 11$ ) Haar [14] wavelet is used. For the original DGPS data (signal),  $s$  consisting of approximately 18 555 data points (i.e.,  $N = 2^n \cong 2^{14}$ ) and sampled at a rate of one measurement per second, there will be approximately 15 ( $n + 1 = 15$ ) wavelet levels available.

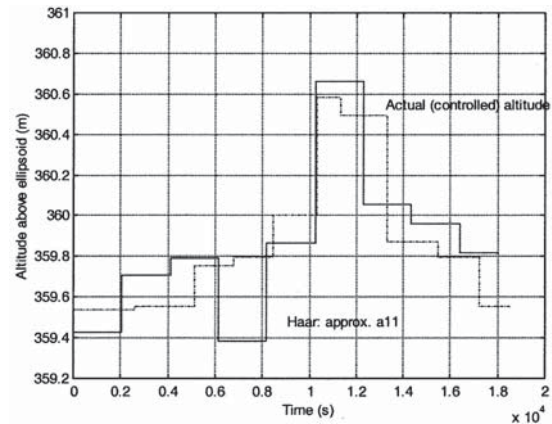


Fig. 4. Comparison of actual altitude measurements with reconstructed HWT approximation,  $a_{11}$ .

It can be seen from Fig. 3 that the trend of the quantitative values of altitudes above ellipsoid in meters of the approximation component,  $a_{11}$  matches that of the original signal,  $s$  to a significant extent. It is to be noted that the shape of the decomposed signal components depends on the shapes of the analyzing wavelet which, in turn, determine the shape of the building blocks from which a particular signal is constructed. Recall that wavelet decomposition of a signal has two main elements: the approximated and the detailed. In Fig. 3, the approximation level is shown as  $a_{11}$  with its associated detailed components as  $d_1$  through  $d_{11}$ . The sum of the various levels results in a signal  $s(t)$  at the top of the Fig. 3. References [13], [14] show how to obtain the approximated and detailed components. For practical purposes, the wavelets toolbox of MATLAB software is used to generate these individual components for the given ten station DGPS measurement data.

## V. QUANTIFICATION OF ERROR

For the purpose of comparing the error resulting from HWT and the previously assessed LSPE method, the approximation component (i.e.,  $a_{11}$ ) of the decomposed DGPS signal has been extracted. Fig. 4 shows the estimated altitude above ellipsoid, resulting from the extracted HWT transform level 11 approximation (i.e.,  $a_{11}$ ) of the decomposed signal and the actual (i.e., controlled) altitude above ellipsoid. As can be seen from Fig. 4, the resulting altitude from  $a_{11}$  closely matches that of the actual or controlled altitudes above ellipsoid. The respective errors or deviations in the LSPE (i.e., error in LSPE) and that of the HWT methods from the actual altitudes are depicted in Fig. 5. For the DGPS altitude data being studied, the HWT approach ( $a_{11}$ ) tends to have relatively better performance than the LSPE in most cases as shown in Fig. 5.

The confidence index resulting from the two selected methods is shown in Figs. 6 and 7. These data are for DGPS measurements taken in the vicinity of 230-kV overhead transmission circuits for a 12-channel receiver. It can be seen that for a 70% confidence level, the  $a_{11}$  component of the HWT presents a lower error of approximately 17.2 cm as opposed to 21.5 cm for the LSPE. Due to the so-called end effect phenomenon in wavelet transform analysis, the accuracy of

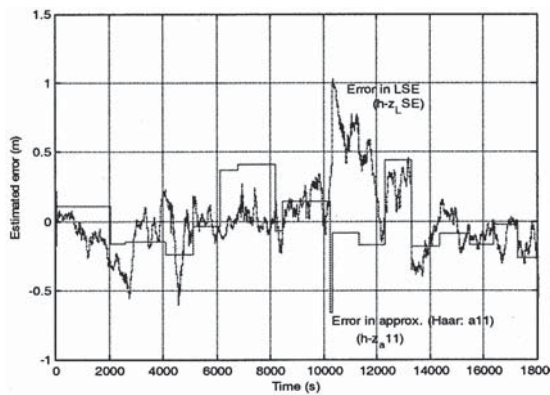


Fig. 5. LSPE versus Haar wavelet errors.

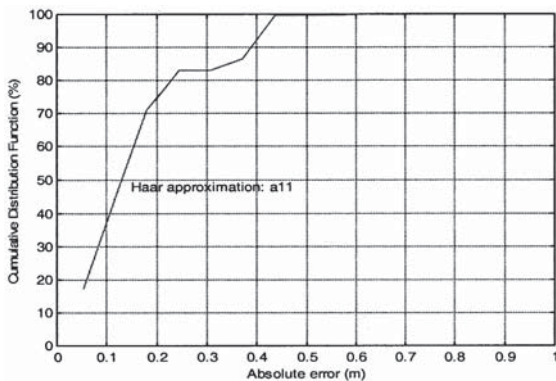


Fig. 6. Cumulative error in altitude ( $z$ ) measurements for HWT ( $a_{11}$ ).

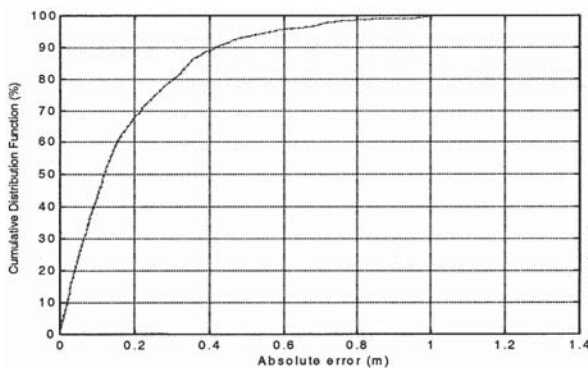


Fig. 7. Cumulative error in altitude ( $z$ ) measurements for LSPE analysis.

the approximated component is distorted. With appropriate curve fitting techniques, it can be seen that the Haar wavelet used in this analysis outperforms the LSPE method. A detailed analysis resulting from the use of bad data identification and modification, artificial neural network estimation (ANNE) and LSPE methods for the same DGPS measurements are given in [1], [18]. A brief summary of the resulting accuracy for selected confidence levels is given in Table IV.

An accurate real-time overhead conductor position ( $x, y, z, t$ ) information can be used to redistribute power flow, detect the extent of conductor movement in the  $x$ - $y$  plane in a remote location. Equally important is the use of overhead conductor sag information for dynamic thermal-line ratings [1], [18]. Corona [19] discharge is a potential source of

TABLE IV  
SELECTED CONFIDENCE LEVELS OF DGPS ALTITUDE MEASUREMENT NEAR 230-kV TRANSMISSION LINES

Confidence Index (%)	Absolute error (cm)		
	HWT approximation ( $a_{11}$ )	ANNE	LSPE
90	30.0*	37.4	41.9
70	17.2	19.6	21.5
60	15.4	14.6	15.4

\*Approximate interpolated value

interference in communication systems in the close proximity of high-voltage environment. Field trial testing conducted in a laboratory environment and at the Ocotillo substation in Tempe, AZ indicates the feasibility of the DGPS signal reception for measurements taken at approximately 14 ft directly below 230-kV lines. However, the severe existence of such a phenomenon (i.e., corona) may affect the normal operation of the DGPS-based conductor sag measurement instrument together with the communication links being used for data transfers. The effect of corona on DGPS measurement in the vicinity of discharges needs further investigation that is beyond the scope of this paper, however, no rover-based radio-communication problems were observed for 902-to-928-MHz (ISM band) technology.

## VI. CONCLUSION

The power engineering applications of GPS technologies, especially those that relate to the measurement of vertical position have been discussed. A DGPS-based conductor sag instrument has been prototyped and is used to measure altitudes.

The LSPE method in combination with bad data identification and correction, and HWT have been used to reduce the error of raw DGPS measurements. One of the main advantages of the wavelet approach is that it does not require initial bad-data identification and modification, a cumbersome filtering process needed for the LSPE method. The results show that the LSPE and HWT approaches exhibit competitive results and reduce the error significantly. The DGPS measurement data accuracy enhancement using the HWT analysis can be considered as a better method. A typical error at the 60% confidence level is 15.4 cm in the DGPS measurements as shown in Table IV.

## REFERENCES

- [1] C. Mensah-Bonsu, U. Fernández Krekeler, G. T. Heydt, Y. Hoverson, J. Schilleci, and B. Agrawal, "Application of the global positioning system to the measurement of overhead power transmission conductor sag," *IEEE Trans. Power Delivery*, vol. 17, pp. 273–278, Jan. 2002.
- [2] U. Fernández, C. Mensah-Bonsu, J. Wells, and G. Heydt, "Calculation of the maximum steady state transmission capacity of a system," in *Proc. 30th N. Amer. Power Symp.*, Cleveland, OH, Oct. 19–20, 1998, pp. 300–305.
- [3] J. Hurn, *Differential GPS Explained*. Sunnyvale, CA: Trimble Navigation Ltd., 1993.
- [4] E. Kaplan, *Understanding GPS: Principles and Applications*. Boston, MA: Artech House, 1996.
- [5] G. T. Heydt, *Computer Analysis Methods for Power Systems*. Scottsdale, AZ: Stars in a Circle Publications, 1998.
- [6] P. Crossley, "Future of the global positioning system in power systems," *Develop. Use Global Positioning Syst.*, pp. 7/1–7/5, 1994.

- [7] G. Harkleroad, W. Tang, and N. Johnson, "Estimation of error correlation distance for differential GPS operation," in *Proc. Position Location Navigation Symp.*, 1990, pp. 378–382.
- [8] T. O. Seppa, "Accurate ampacity determination: Temperature sag model for operational real time ratings," *IEEE Trans. Power Delivery*, vol. 10, pp. 1460–1470, July 1995.
- [9] H. Pohlmann and R. Thomas, "Sag increases resulting from conductor creep on medium-voltage transmission lines, and the problem of measuring sag on live overhead lines," in *Twelfth International Conference on Electricity Distribution*. Brussels, Belgium: CIRED, 1993, vol. 3, pp. 3.20/1–5.
- [10] D. A. Douglas and A.-A. Edris, "Field studies of dynamic thermal rating methods for overhead lines," in *Proc. 1999 IEEE Trans Dist. Conf.*, vol. 2, 1999, pp. 842–851.
- [11] W. Z. Black and W. R. Byrd, "Real-time ampacity model for overhead lines," *IEEE Trans. Power App. Syst.*, vol. PAS-102, pp. 2289–2293, July 1983.
- [12] T. H. Koornwinder, *Wavelets: An Elementary Treatment of Theory and Applications*. River Edge, NJ: World Scientific Publishing, 1993.
- [13] D. E. Newland, *An Introduction to Random Vibrations, Spectral and Wavelet Analysis*, Third ed. London, UK: Longman Group, 1993.
- [14] M. Misiti, Y. Misiti, G. Oppenheim, and J.-M. Poggi, *Users Guide: Wavelet Toolbox for Use With MATLAB*. Natick, MA: The MathWorks, Inc., 1997.
- [15] W. A. Wilkinson and M. D. Cox, "Discrete wavelet analysis of power system transients," *IEEE Trans. Power Syst.*, vol. 11, pp. 2038–2044, Nov. 1996.
- [16] G. T. Heydt and A. W. Galli, "Transient power quality problems analyzed using wavelets," *IEEE Trans. Power Delivery*, vol. 12, pp. 908–915, Apr. 1997.
- [17] C. K. Chui, *An Introduction to Wavelets*. New York: Academic, 1992.
- [18] C. Mensah-Bonsu, "Instrumentation and measurement of overhead conductor sag using the differential global positioning satellite system," Ph.D. dissertation, Arizona State Univ., Tempe, Aug. 2000.
- [19] E. Kuffel and W. S. Zaengl, *High Voltage Engineering Fundamentals*. New York: Pergamon, 1984.
- [20] J. K. Neter, C. J. Nachtsheim, and W. Wasserman, *Applied Linear Statistical Models*, 4th ed. Chicago, IL: Times Mirror Higher Education Group, 1996.
- [21] Anonymous, "Satellite pictures: Private eyes in the sky," *Economist*, pp. 71–73, May 6, 2000.

**Chris Mensah-Bonsu** (S'96–M'00) received the Ph.D. degree in electrical engineering from Arizona State University, Tempe.

He is presently with the Market Operations Group, California Independent System Operator (ISO) as a Market Design Engineer. His research interests are in the areas of power systems, dynamic thermal-line rating, and system reliability issues pertaining to the competitive electricity market environment.

**Gerald Thomas Heydt** (F'91) received the Ph.D. degree in electrical engineering from Purdue University, West Lafayette, IN.

He is presently a Professor of electrical engineering at Arizona State University, Tempe. He is also the author of two books on electric power engineering.

Dr. Heydt received the 1995 Power Engineering Society "Power Engineering Educator of the Year" award. He is a member of the National Academy of Engineering.